Marine Environmental Research 179 (2022) 105699

Contents lists available at ScienceDirect

Marine Environmental Research

journal homepage: www.elsevier.com/locate/marenvrev

Concentrations of transparent exopolymer particles (TEPs) and their role in the carbon export in the South China Sea and western tropical North Pacific

Shujin Guo [a,b,c], Ying Wu [d], Mingliang Zhu [a,b,c], Xiaoxia Sun [a,b,c,e,*]

[a] Jiaozhou Bay National Marine Ecosystem Research Station, Institute of Oceanology, Chinese Academy of Sciences, Qingdao, 266071, PR China
[b] Laboratory for Marine Ecology and Environmental Science, Pilot National Laboratory for Marine Science and Technology (Qingdao), Qingdao, 266237, PR China
[c] Center for Ocean Mega-Science, Chinese Academy of Sciences, Qingdao, 266071, PR China
[d] State Key Laboratory of Estuarine and Coastal Research, East China Normal University, Shanghai, 201100, PR China
[e] University of Chinese Academy of Sciences, Beijing, 100049, PR China

ARTICLE INFO

Keywords:
Transparent exopolymer particles
Distribution
Environmental factors
Carbon
Sinking flux
South China Sea
Western tropical north pacific

ABSTRACT

The role of TEPs in the carbon cycle remains inadequately understood in oligotrophic tropical oceans. This study investigates TEP concentrations, distributions, sinking behavior and fluxes in the oligotrophic South China Sea (SCS) and western tropical North Pacific (WTNP). The results suggested that TEPs levels were relatively low [< 60 μg Xeq. L^{-1} (μg xanthan gum equivalent per liter)] in both regions, and they were higher in the epipelagic layer than in deeper layers. TEP concentrations correlated significantly positively with Chl *a* and picophytoplankton biomass, and TEP-associated carbon contributed significantly to particulate organic carbon (POC) pool in the SCS and WTNP. The sinking flux of TEPs constituted a mean of 61% of the total POC flux in the SCS and 46% in the WTNP, highlighting their important role in carbon export in these areas. Generally, this study should provide good insight into the role TEPs play in the carbon cycle in oligotrophic tropical oceans.

1. Introduction

Transparent exopolymer particles (TEPs) are organic gel-like and polysaccharide-enriched particles (from ~0.4 to >200 μm) with a ubiquitous distribution in the ocean (Alldredge et al., 1993; Li et al., 1998; Passow, 2002a). Phytoplankton, including diatoms, dinoflagellates, coccolithophores, cyanobacteria and cryptomonads, are considered the main TEP producers in the ocean (Passow, 2002a; Nissimov et al., 2018; Ortega-Retuerta et al., 2019). The production of TEPs by marine phytoplankton is mainly influenced by phytoplankton abundance (Passow, 2002a), species composition (Fukao et al., 2012) and physiological status (Morelle et al., 2017). Moreover, TEP dynamics can be affected by a variety of environmental factors, such as temperature, nutrient availability, cation ions, and turbulence (Pedrotti et al., 2010; Fukao et al., 2012; Sun et al., 2012; Burns et al., 2019). Several other organisms, such as bacteria, zooplankton, and benthic feeders, can also produce TEPs in the ocean (Prieto et al., 2001; Shackelford and Cowen, 2006; Sugimoto et al., 2007; Heinonen et al., 2007).

As the density of pure TEPs ranges from 0.70 to 0.84 g cm^{-3}, which is lower than that of seawater (Azetsu-Scott and Passow, 2004), freshly produced, particle-free TEPs would show an upward trend in the water column in the ocean (Mari et al., 2017). However, TEPs can be easily ballasted by other heavier organic and mineral components (e.g., phytoplankton cells, clay, calcium carbonate) due to their sticky nature, which further generates larger aggregates with high density in the ocean (Passow and Alldredge, 1995b; Beauvais et al., 2006; Ploug and Passow, 2007; Liu et al., 2021a). The ballasted TEPs can then sink down to the sea bottom (Koeve, 2005; Martin et al., 2011). As the carbon content of TEPs is high (Engel and Passow, 2001), the ability to increase aggregate formation and subsequent sinking of TEPs indicate that they should be important in the carbon cycle in the ocean (Mari et al., 2017).

Several studies have found that TEP sinking can be relevant to carbon accumulation in the deep ocean, with TEPs accounting for 8–14% of particulate organic carbon (POC) flux at 200 m in the subarctic Pacific (Ramaiah et al., 2005) and 24–78% of POC fluxes in the 300 m layer in the Gulf of Aqaba (Bar-Zeev et al., 2009). In the subpolar North Atlantic, 25–43% of the TEP-associated particulate carbon at the 100 m depth was found to export below 750 m (Martin et al., 2011). Most of these studies on TEP sinking have been carried out in high latitude oceanic regions, and there has been limited information on TEP sinking behavior

* Corresponding author. Jiaozhou Bay National Marine Ecosystem Research Station, Institute of Oceanology, Chinese Academy of Sciences, 7 Nanhai Road, Shinan District, Qingdao, 266071, PR China.
E-mail address: xsun@qdio.ac.cn (X. Sun).

https://doi.org/10.1016/j.marenvres.2022.105699
Received 18 April 2022; Received in revised form 29 June 2022; Accepted 7 July 2022
Available online 9 July 2022

and its contribution to carbon export in oligotrophic tropical oceans (Ge et al., 2022). Oligotrophic tropical oceans constitute an important part of the global ocean and play an important role in the global oceanic carbon cycle (Palmer and Totterdell, 2001; Christian et al., 2008). Through biological pumps, the oligotrophic tropical ocean can deposit atmospheric carbon dioxide to the deep ocean (Moutin et al., 2008), and the study of TEP concentrations and their sinking behavior in these regions would be beneficial for predicting the carbon flow in oligotrophic tropical oceans.

The South China Sea (SCS) and western tropical North Pacific (WTNP) are two typical oligotrophic tropical oceans. Both N and P in the euphotic layer of the SCS are usually below the detectable limits, and chlorophyll (Chl) *a* concentrations are also low (Chen et al., 2011; Xiao et al., 2015; Liu et al., 2017). WTNP is also a famous oligotrophic region with Chl *a* concentrations lower than 0.25 μg L^{-1} (Messié and Radenac, 2006; Kodama et al., 2014), and the phytoplankton community structure in the WTNP is mostly dominated by picophytoplankton (Liu et al., 2021b; Ma et al., 2021). Until now, there have been few studies on the TEP concentration and distribution in the SCS and WTNP (Kodama et al., 2014; Yamada et al., 2017; Ge et al., 2022), and the knowledge on TEP sinking behavior and its contribution to carbon export is still quite limited in these areas. In this study, samples were collected in the SCS and WTNP during two cruises in 2017 and 2019, and the concentrations of TEPs and their controlling factors were studied. The sinking velocity of TEPs and their contribution to carbon export were also determined. The main goals of this study were to (1) determine the concentrations of TEPs in the SCS and WTNP, clarify their distribution patterns and their biotic and abiotic drivers and (2) determine their sinking flux and clarify the role TEPs play in carbon export in these regions. This study should provide useful information for understanding the participation of TEPs in the carbon cycle in oligotrophic tropical oceans.

2. Materials and methods

2.1. Study area and sampling stations

Seawater samples were collected in the SCS slope onboard the RV 'Nanfeng' (15 March to 2 April 2017) and in the WTNP onboard the RV 'Ke Xue' (13 November to 10 December 2019) (Fig. 1). Eight stations in both the SCS and WTNP were selected to collect seawater samples (Table 1).

2.2. Sampling and analysis

2.2.1. Environmental parameters

Water temperature and salinity were determined with a conductivity, temperature and depth (CTD, model: SBE 9plus, Seabird) sensor. Seawater samples for the measurement of nutrients, Chl *a*, TEPs and other biological parameters were collected with Niskin bottles mounted on the CTD, and 5–7 layers from the 5–220 m depth were sampled at each station. Samples for POC analysis were collected in each layer with CTD at stations L3, L5, L12 and L13 in the SCS and stations E4, E6, E19 and E21 in the WTNP.

Seawater for dissolved inorganic nutrient analysis was collected and filtered through a 0.45 μm pore-size cellulose acetate membrane, and the filtrates were stored below −20 °C until analysis. In the lab, the samples were processed and analyzed with a Technicon AA3 auto-analyzer (Bran-Lube, GmbH) (Han et al., 2012). The detection limits for nutrients were 0.02 μmol L^{-1} for NO_3^-, 0.02 μmol L^{-1} for NO_3^-, 0.03 μmol L^{-1} for PO_4^{3-} and 0.05 μmol L^{-1} for SiO_3^{2-}. Chl *a* was determined with the fluorimetric method (Welschmeyer, 1994). Seawater samples (500 mL) were filtered through 0.7 μm Whatman GF/F filters and then extracted in 90% acetone for 24 h in the dark at 4 °C until processing in a Turner Design fluorometer (Turner Designs Model 10).

2.2.2. Phytoplankton and heterotrophic prokaryote (HP) analysis

Seawater samples for phytoplankton analysis were fixed with formaldehyde solution (2% final formalin concentration) in polyethylene bottles aboard. Upon return to the lab, a 100 mL sample was allowed to settle for 24–48 h in sedimentation chambers (Hydrobios, Kiel, Germany), and phytoplankton cells (>2 μm) were then identified and enumerated with an inverted microscope (Olympus CKX41) at 200 × or 400 × magnification (Utermöhl, 1958). The linear dimensions of phytoplankton cells were measured, and the cell volume was then calculated using geometric models (Hillebrand et al., 1999). At least twenty cells were measured for each phytoplankton species for their linear dimensions. The cell C content of phytoplankton was calculated using the recommended conversion equations of Menden-Deuer and Lessard (2000). Samples for picophytoplankton (<2 μm) analysis (4.5 mL) were fixed with 1% paraformaldehyde plus 0.05% glutaraldehyde and then frozen in liquid nitrogen at −80 °C. Upon return to the lab, samples were analyzed with a FACS Calibur (Becton and Dickinson) flow cytometer. Three groups of picophytoplankton (*Synechococcus*, *Prochlorococcus* and picoeukaryotes) were distinguished and enumerated. The cell C content of picophytoplankton was calculated using the conversion factors of Zamanillo et al. (2019a): 175 fg C $cell^{-1}$ for *Synechococcus*, 51 fg C $cell^{-1}$ for *Prochlorococcus* and 1319 fg C $cell^{-1}$ for picoeukaryotes. It should be noted that uncertainty sources for the carbon estimation in this study were biovolume estimates and conversion factors.

HPs were determined with the same fixing method and instrument for picophytoplankton described above. In the lab, samples were thawed

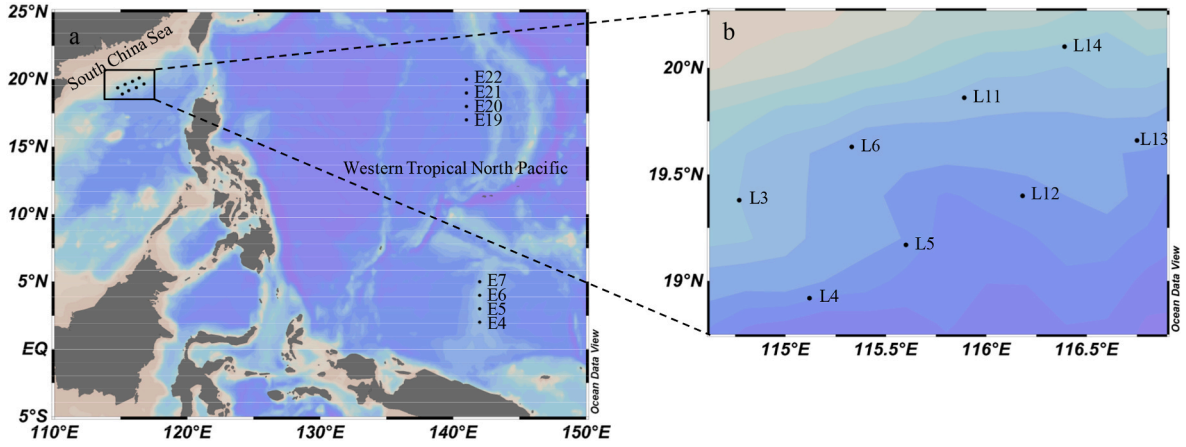

Fig. 1. Sampling stations in the SCS in 2017 and WTNP in 2019. a: general view of the study area and sampling stations; b: enlarged view of the sampling stations in the SCS.

Table 1
Physical and chemical properties of the surface layers of the sampling stations in the SCS and WTNP. PSU, practical salinity unit; –, under detection limit.

	St.	Longitude (E)	Latitude (N)	Bottom depth(m)	Temperature (°C)	Salinity (PSU)	NO_3^- (μmol L^{-1})	NO_2^- (μmol L^{-1})	PO_4^{3-} (μmol L^{-1})	SiO_3^{2-} (μmol L^{-1})	Chl *a* (μg L^{-1})	TEP(μg Xeq. L^{-1})
SCS	L3	114°46′08″	19°22′47″	1280	26.38	33.33	0.02	–	0.01	2.24	0.11	41
	L4	115°07′21″	18°55′02″	2800	25.43	34.02	–	0.01	0.01	2.25	0.01	25
	L5	115°36′11″	19°10′03″	2700	25.27	34.64	0.02	–	0.03	1.82	0.01	21
	L6	115°19′55″	19°37′32″	2033	24.61	34.63	–	–	0.04	1.83	0.01	33
	L11	115°52′22″	19°50′51″	1514	24.73	34.70	0.06	0.01	0.01	1.62	0.09	30
	L12	116°10′56″	19°23′42″	1969	25.13	34.70	–	0.01	0.01	1.69	0.11	30
	L13	116°44′50″	19°39′46″	2017	24.71	34.66	0.02	–	0.02	1.72	0.10	26
	L14	116°23′10″	20°06′10″	993	25.01	34.48	0.03	–	0.02	2.01	0.10	36
WTNP	E4	142°00′00″	2°00′00″	2559	29.36	34.21	0.27	0.05	0.26	0.69	0.08	35
	E5	142°00′00″	3°00′00″	2352	29.23	34.30	0.16	0.03	0.78	3.03	0.07	29
	E6	142°00′00″	4°00′00″	2453	29.56	34.07	0.06	0.04	0.18	0.73	0.05	22
	E7	142°00′00″	5°00′00″	2618	29.26	34.06	0.85	0.07	0.16	1.34	0.12	32
	E19	141°00′00″	17°00′00″	4782	28.63	34.50	0.06	0.03	0.11	1.16	0.07	21
	E20	141°00′00″	18°00′00″	4710	28.48	34.44	0.02	0.03	0.15	1.25	0.05	21
	E21	141°00′00″	19°00′00″	4645	28.62	34.30	0.09	0.05	0.14	1.44	0.06	26
	E22	141°00′00″	20°00′00″	4608	28.63	34.31	0.06	0.04	0.14	1.28	0.06	28

and stained with SYBR Green I (Molecular Probes) at a final concentration of 10 μM. Ten microliters per sample of a 10^5 mL^{-1} solution of yellow–green 0.92 μm Polysciences latex beads were added as an internal standard, and the samples were analyzed with a flow cytometer. The carbon content of the HPs (HP–C) was calculated using a conversion factor of 12.3 fg C $cell^{-1}$ (Ducklow, 2000).

2.2.3. TEP and POC analyses

TEP concentrations were determined using the classical method of Passow and Alldredge (1995a). Triplicate 500 mL seawater samples were gently filtered (<150 mmHg) through 0.4 μm pore size polycarbonate filters (25 mm diameter, Whatman) and then stained with 1 ml of Alcian Blue solution (8 GX; Sigma–Aldrich) in 0.06% v/v acetic acid (pH 2.5). The filters were rinsed with 2 mL of Milli-Q water, and then the Alcian Blue-stained material in the filters was extracted with 6 mL of 80% sulfuric acid for 3 h. The absorbance of the extracted material was measured spectrophotometrically at 787 nm using a Varian Cary spectrophotometer (Metash, Shanghai, China). For the measurement of filter blanks, empty filters stained with Alcian Blue were also prepared with every batch of samples. For TEP concentration calculation, the mean filter blank value was first subtracted from the absorbance for the seawater samples, and the TEP concentration was then calculated by a standard curve prepared with xanthan gum according to Passow and Alldredge (1995a). TEP concentrations were expressed in micrograms of μg xanthan gum equivalent per liter (μg Xeq. L^{-1}). The detection limit of the technique was 5 μg Xeq. L^{-1}, and the standard deviation in replicate samples was <20%. The carbon associated with the TEPs (TEP-C) was calculated using a conversion factor of 0.51 μg C μg Xeq. L^{-1} (Engel and Passow, 2001).

POC was determined by filtering 6 L of seawater on precombusted GF/F glass fiber filters (0.7 μm pore size, 4 h, 450 °C). The filters were then stored frozen (−20 °C) until analysis. Prior to analysis, the filters were dried at 60 °C for 24 h and then placed in an HCl-saturated atmosphere to remove inorganic carbon. Finally, the filters were dried again and analyzed in a C:H:N autoanalyzer by high temperature (900 °C) combustion (Perkin-Elmer 240).

2.2.4. TEP sinking velocity and sinking flux

To clarify the sinking behavior of TEP excluding the effect of seawater turbulence, the sinking velocities of TEPs were determined at stations L3, L5, L12, and L13 in the SCS and E4, E6, E19, and E21 in the WTNP with the settling column (SETCOL) method (Bienfang, 1981), which has been used in other studies (Azetsu-Scott and Passow, 2004; Mari, 2008; Guo et al., 2021). For analysis, a Plexiglass column (height = 1 m, volume = 7.85 L) was filled completely with a homogeneous seawater sample immediately after sampling, and it was allowed to settle undisturbed for 2–3 h. Finally, the seawater in the upper, middle, and bottom compartments of the column was successively drained via taps in the column wall. TEP concentration in all three compartments was measured before and after settlement, and the sinking velocity of TEPs was calculated according to the formula:

$$V = (B_s/B_t) \times L/t, \quad \text{(Eq.1)}$$

where V = sinking velocity; B_s = TEP amount settled into the bottom compartment of the column; B_t = total TEPs amount in the column; L = length of the column; and t = settling interval. Sinking velocities were determined at the surface (5 m), deep Chl *a* maximum (DCM) layer and 200 m layer, and triplicate plexiglass columns were set at each layer.

A sediment trap was deployed during the daytime in the 200 m layer for approximately 12–24 h at stations L3, L5 and L12 in the SCS and stations E4, E6, E19 and E21 in the WTNP. The trap was hung with a crane of the vessel, and a 30 kg lead fish was hung bottom to ensure the vertical stability of the trap. The trap was composed of two-plexiglass cylinders (height: diameter = 80 cm: 10 cm). The trap mouths were covered with honeycomb baffles. On recovery, buffered formaldehyde (5% final concentration) was added to each cup, and then the sample from each cup was split using a rotary splitter for analysis of TEP and POC. After returning to the lab, two aliquots (700 ml) of each cup were filtered with a glass fiber filter (Whatman GF/F) for analysis of POC, and two aliquots (300 ml) were filtered with 0.4 μm pore size polycarbonate filters (25 mm diameter, Whatman) for analysis of TEP. From the TEP and POC concentrations determined in the trap, TEP and POC sinking fluxes (mg C m^{-2} d^{-1}) were estimated by considering the sample volume in the trap, surface area of the trap, and duration of trap exposition (Vicente et al., 2009).

2.3. Data analysis

Pearson correlation analysis was used to analyze the relationship between TEP concentrations and various environmental parameters using SPSS 14.0 software. A *t-test* was used to verify the significant differences between two groups of data, and the significance level was set at $p < 0.05$.

3. Results

3.1. Hydrological conditions

In the SCS, sea surface temperatures ranged from 24.61 °C to 26.38 °C, and sea surface salinity ranged from 33.33 to 34.70. Thermal stratification was observed in this area (Fig. 2a and b). Nitrate was

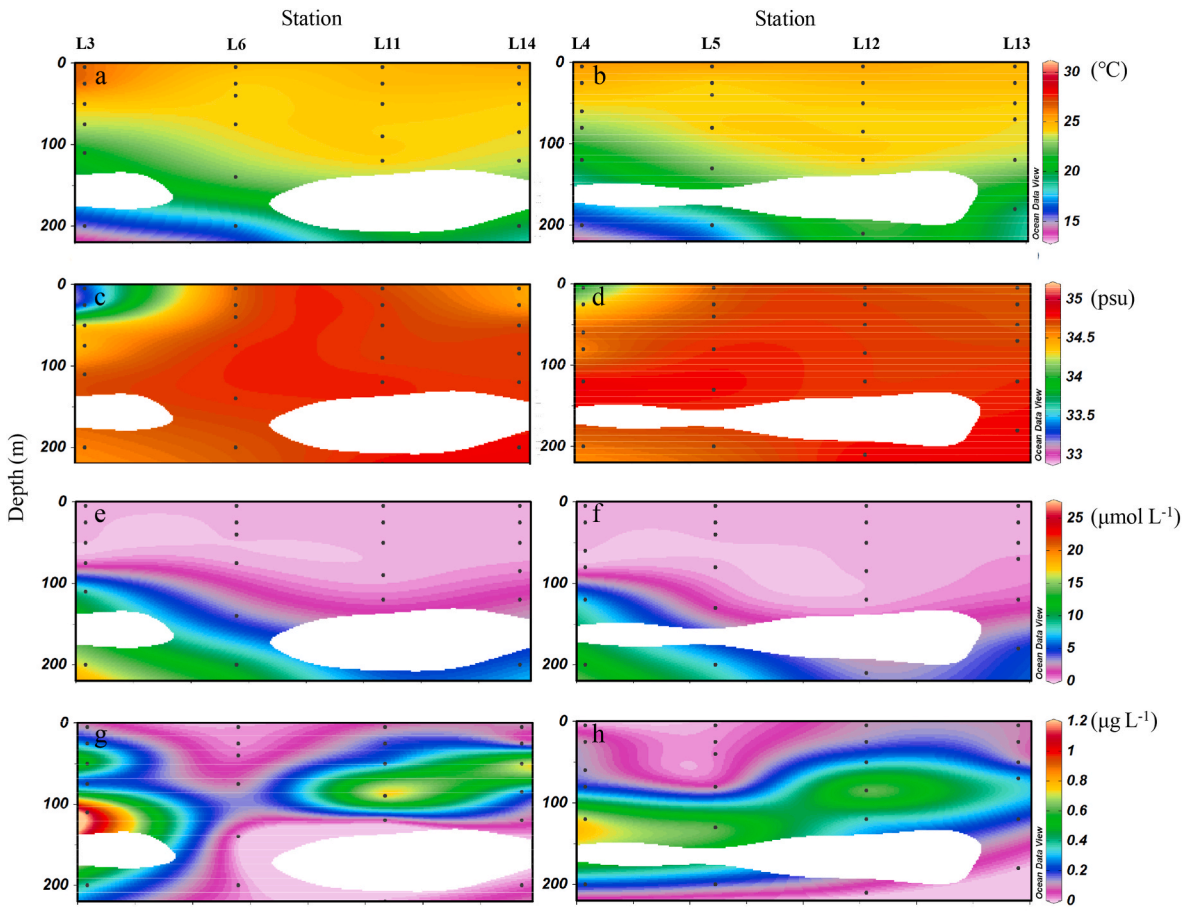

Fig. 2. Sectional distributions of temperature (°C) (a, b), salinity (psu) (c, d), nitrate (μmol L^{-1}) (e, f) and Chl *a* (μg L^{-1}) (g, h) in the SCS.

generally depleted in the upper 120 m layers, and the concentration obviously increased with increasing depth (Fig. 2e and f). The surface Chl *a* concentration ranged from 0.01 μg L^{-1} to 0.11 μg L^{-1} (mean = 0.07 ± 0.04 μg L^{-1}). The DCM layer was observed from the 75 m–120 m layer at the sampling stations (Fig. 2g and h), with Chl *a* concentrations ranging from 0.09 μg L^{-1} to 1.13 μg L^{-1} (mean = 0.62 ± 0.29 μg L^{-1}). In the WTNP, strong column stratification was also observed at all sampling stations (Fig. 3a and b). Sea surface temperatures ranged from 28.48 °C to 29.56 °C, and sea surface salinity ranged from 34.06 to 34.50. Similar to the SCS, the WTNP was characterized by quite low nitrate concentrations in the epipelagic layer (Fig. 3e and f). The mean sea surface Chl *a* concentration was 0.06 ± 0.02 μg L^{-1}, and DCM was observed from the 50–120 m layer (Fig. 3g and h), with Chl *a* concentrations ranging from 0.10–0.44 μg L^{-1} (mean = 0.23 ± 0.10 μg L^{-1}). In both regions, nutrient concentrations in the surface mixed layer and DCM layer were lower than those in the deeper layer, while Chl *a* concentrations were higher in the surface mixed layer and DCM layer (Table 2).

3.2. TEP concentrations and TEP-C

TEP concentrations varied between 14 and 47 μg Xeq. L^{-1} (mean = 30 ± 8 μg Xeq. L^{-1}) in the SCS and 12 and 54 μg Xeq. L^{-1} (mean = 34 ± 10 μg Xeq. L^{-1}) in the WTNP (Fig. 4). The TEP concentration had a maximum value between the 50 and 85 m layer and a minimum value between the 180 and 220 m layer in the SCS (Fig. 4a and b). In the WTNP, the maximum TEP concentration was observed between the 50 and 120 m layers (Fig. 4c and d). Generally, TEP concentrations in the upper 120 m layer were significantly higher than those in the deeper layer in the SCS (n = 48, *t*-test, $p < 0.05$) and WTNP (n = 53, *t*-test, $p < 0.05$) (Fig. 4). TEPs correlated significantly and positively with temperature, Chl *a* and picophytoplankton biomass and significantly and negatively with NO_3^-, PO_4^{3-} and SiO_3^{2-} concentrations (Table 3). No significant correlation was observed between TEP and HP. The inventories of TEP and Chl *a* in the upper 220 m of each station were also calculated, and the ratio of TEP to Chl *a* ranged from 52 to 410 μg Xeq. μg Chl a^{-1} (mean = 157 ± 101 μg Xeq. μg Chl a^{-1}) in the SCS and 244–584 μg Xeq. μg Chl a^{-1} (mean = 372 ± 99 μg Xeq. μg Chl a^{-1}) in the WTNP.

TEP-C ranged from 7 to 24 μg C L^{-1} (mean = 16 ± 4 μg C L^{-1}) in the SCS and 6–28 μg C L^{-1} (mean = 15 ± 4 μg C L^{-1}) in the WTNP, and it constituted 32%–173% (mean = 75 ± 37%) of the total POC in the SCS and 45%–114% (mean = 61 ± 40%) of the POC in the WTNP. In both regions, TEP-C contributed the most to the POC pool, followed by phyto-C (35 ± 21% in the SCS and 41 ± 27% in the WTNP), and HP-C contributed the least (15 ± 6% in the SCS and 25 ± 14% in the WTNP) (Fig. 5).

3.3. SETCOL-determined sinking velocities and sinking fluxes of TEPs

The sinking velocities of TEPs determined with the SETCOL method ranged from 0.11 to 0.93 m d^{-1} (mean = 0.49 ± 0.24 m d^{-1}) in the SCS and 0.09–0.63 m d^{-1} (mean = 0.36 ± 0.16 m d^{-1}) in the WTNP. Generally, SETCOL-determined sinking velocities of TEPs were significantly higher in the DCM layer than in the surface and 200 m layers (*t*-test, $p < 0.05$) (Fig. 6). The sinking flux of TEPs averaged 13 mg C m^{-2} d^{-1} in the SCS and 12 mg C m^{-2} d^{-1} in the WTNP (Fig. 7). Overall, sinking TEPs constituted a mean of 61% and 46% of the total POC sinking flux in the SCS and WTNP, respectively.

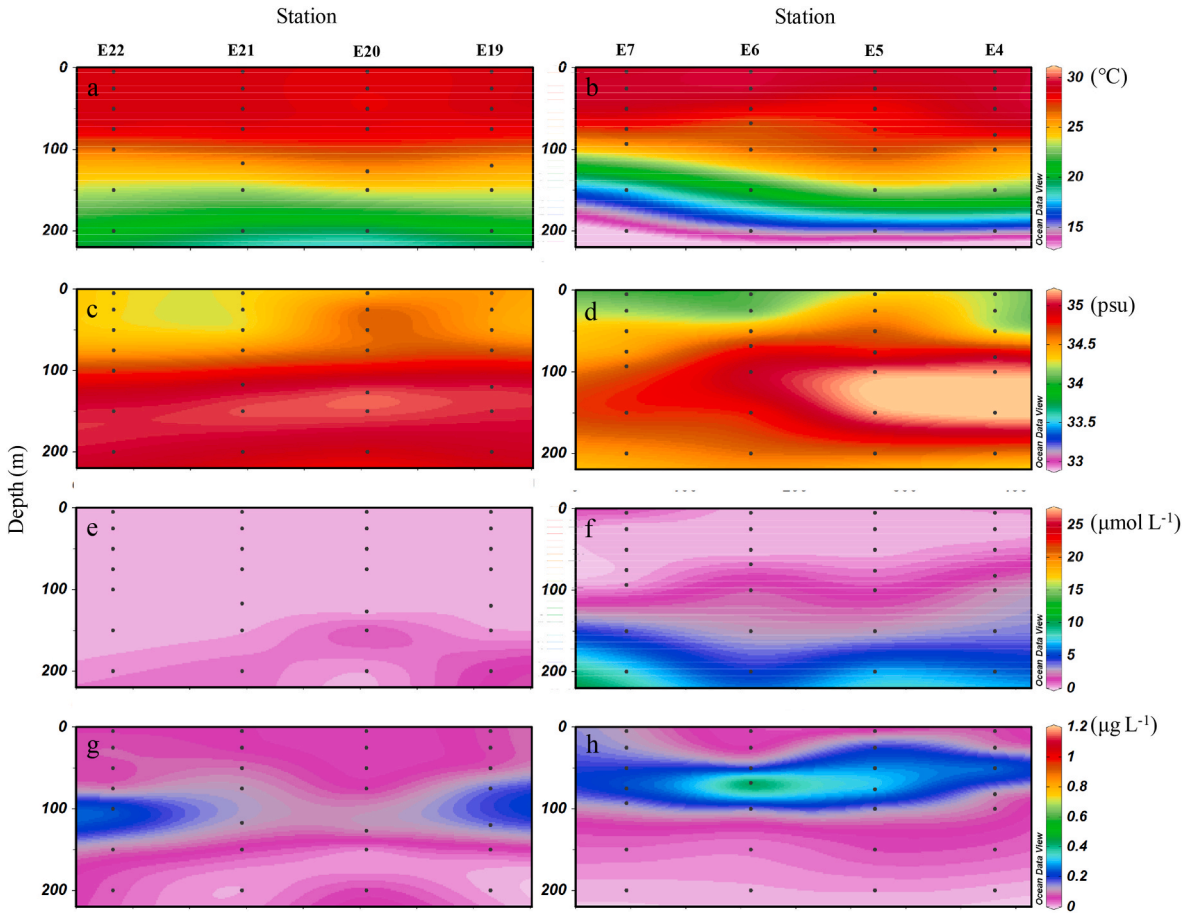

Fig. 3. Sectional distributions of temperature (°C) (a, b), salinity (psu) (c, d), nitrate (μmol L^{-1}) (e, f) and Chl *a* (μg L^{-1}) (g, h) in the WTNP.

Table 2
Environmental parameters and TEP concentrations (mean values ± standard deviation) in the surface mixed layer, DCM layer and lower layers (layers deeper than DCM) in the SCS and WTNP.

Region	Layer	Temperature (°C)	Salinity (psu)	NO_3^- (μmol L^{-1})	PO_4^{3-} (μmol L^{-1})	SiO_3^{2-} (μmol L^{-1})	Chl *a* (μg L^{-1})	TEP (μg Xeq. L^{-1})
SCS	Surface mixed layer	24.56 ± 0.73	34.50 ± 0.38	0.04 ± 0.11	–	1.85 ± 0.31	0.13 ± 0.11	34 ± 7
	DCM	23.07 ± 1.40	34.74 ± 0.05	2.14 ± 3.19	0.13 ± 0.15	3.47 ± 2.82	0.62 ± 0.29	32 ± 4
	Lower layer	20.56 ± 3.08	34.73 ± 0.07	5.21 ± 4.73	0.35 ± 0.31	7.09 ± 6.13	0.13 ± 0.13	23 ± 7
WTNP	Surface mixed layer	28.77 ± 0.42	34.38 ± 0.17	0.10 ± 0.16	0.17 ± 0.13	1.21 ± 0.60	0.09 ± 0.05	33 ± 6
	DCM	27.19 ± 1.20	34.72 ± 0.24	0.26 ± 0.21	0.15 ± 0.04	1.15 ± 0.37	0.23 ± 0.10	47 ± 4
	Lower layer	21.66 ± 4.24	34.92 ± 0.21	2.20 ± 2.20	0.31 ± 0.18	2.93 ± 3.00	0.06 ± 0.05	30 ± 10

–: under detection limit.

4. Discussion

4.1. Comparison of TEP concentrations in this study with other studies

Compared to eutrophic coastal waters, studies on TEP concentrations in oligotrophic oceans are limited, with several reports in the North Atlantic Ocean (Engel, 2004; Jennings et al., 2017), South Atlantic Ocean (Zamanillo et al., 2019a), northern South China Sea (Ge et al., 2022), North Pacific Ocean (Kodama et al., 2014; Yamada et al., 2017) and Eastern Indian Ocean (Guo et al., 2021) (Table 4). TEP concentrations ranged from 12 to 54 μg Xeq. L^{-1} in this study, which were lower than those reported in a coastal frontal zone of the northern SCS (35–161 μg Xeq. L^{-1}, Li et al., 2021) and the Pearl River estuary (89–1727 μg Xeq. L^{-1}, Sun et al., 2012), but were quite similar to previous reports in the North Pacific (18–69 μg Xeq. L^{-1}, Kodama et al., 2014; 5–40 μg Xeq. L^{-1}, Yamada et al., 2017) and the Eastern Indian Ocean (18–69 μg Xeq. L^{-1}, Guo et al., 2021). Coastal seas are directly influenced by river nutrient inputs, leading to high phytoplankton growth rates and biomass there, which would result in higher TEP levels there (Guo and Sun, 2019).

For a better comparison among different oceanic ecosystems, the ratio between the TEP and Chl *a* inventories in the upper 220 m was also examined. The ratio of TEP: Chl *a* inventories in the upper 220 m averaged 157 ± 101 μg Xeq. μg Chl a^{-1} in the SCS and 372 ± 99 μg Xeq. μg Chl a^{-1} in the WTNP in this study, which were higher than those reported in several coastal seas, such as the Ross Sea (85 μg Xeq. μg Chl a^{-1}, Engel, 2004) and Bransfield Strait, Antarctica (51 μg Xeq. μg Chl a^{-1}, Corzo et al., 2005). The relatively high TEP: Chl *a* ratio in the SCS and WTNP was possibly due to nutrient scarcity there. Several studies have found that the production of phytoplankton extracellular carbohydrates is higher under nutrient stress (Obernosterer and Herndl, 1995; Underwood et al., 2004). When irradiance is not limiting, insufficient inorganic nutrients may limit phytoplankton biomass but not photosynthesis, and the surplus carbon produced by phytoplankton cells

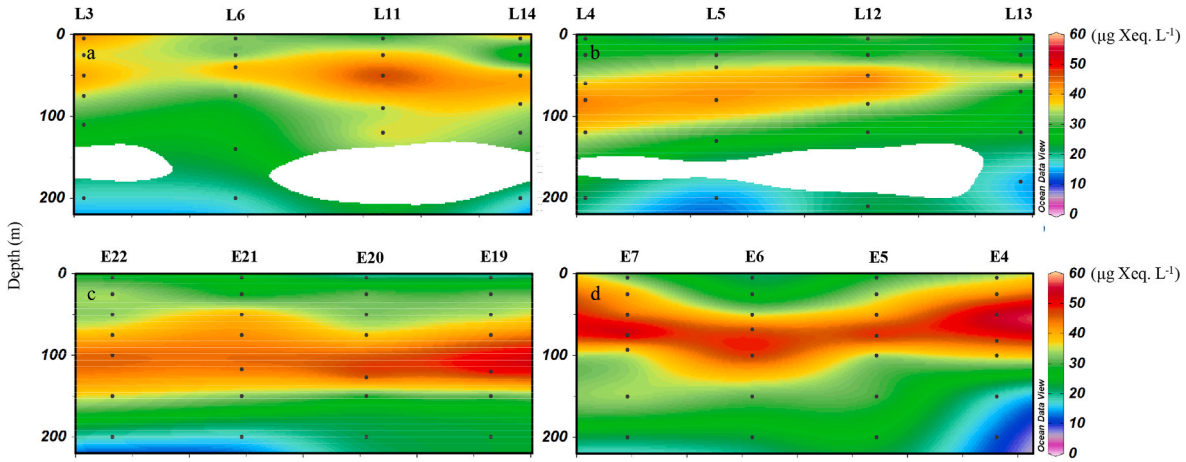

Fig. 4. Sectional distributions of TEP concentrations (μg Xeq. L^{-1}) in the SCS (a, b) and WTNP (c, d).

Table 3
Pearson's correlation coefficients and 2-tailed significance matrix for TEPs and physical, chemical and biological parameters in the SCS and WTNP. T: temperature; HP: heterotrophic prokaryote abundance.

Cruise		T	NO_3^-	PO_4^{3-}	SiO_3^{2-}	Chl *a*	Phyto-C (>2 μm)	Phyto-C (≤2 μm)	HP
SCS	R(p, 2-tailed)	0.59[b]	−0.57[b]	−0.57[b]	−0.52[b]	0.22[a]	−0.67	0.35[a]	0.72
		0.00	0.00	0.00	0.00	0.04	0.49	0.03	0.29
	N	48	48	48	48	48	38	38	30
WTNP	R (p, 2-tailed)	0.47[b]	−0.37[b]	−0.34[a]	−0.33[a]	0.73[b]	0.27	0.78[b]	0.11
		0.00	0.01	0.01	0.01	0.00	0.17	0.00	0.34
	N	56	56	56	56	56	41	41	35

[a] Correlation is significant at the 0.05 level (2-tailed).
[b] Correlation is significant at the 0.01 level (2-tailed).

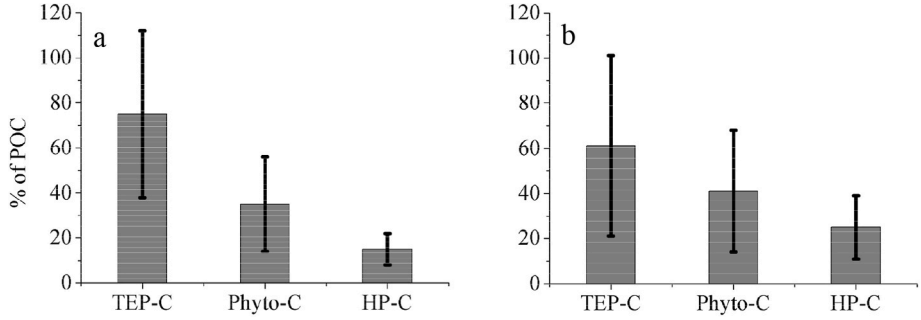

Fig. 5. Relative contributions of TEP-C, Phyto-C and HP-C to the total POC pool in the SCS (a) and WTNP (b).

would be exuded as extracellular carbohydrates, accelerating the formation of TEPs in seawater (Pedrotti et al., 2010). Furthermore, bacterial metabolism is slowed down under limited inorganic nutrient concentrations (Obernosterer and Herndl, 1995), and TEPs produced by phytoplankton may not be efficiently utilized by heterotrophic bacteria under these conditions, further resulting in high TEP: Chl *a* ratios in the study area.

4.2. Main drivers of TEP concentrations and distribution

To better understand the distribution of TEPs in the ocean, it is important to clarify their relationship with various environmental modulators. In this study, significant positive correlations were observed between TEP and Chl *a* in both regions (Table 3), suggesting that phytoplankton should be important TEP producers in the study area. The phytoplankton community structure in the SCS and WTNP was mostly dominated by picophytoplankton (Chen et al., 2011; Liu et al., 2017; Dai et al., 2020). Several studies have reported the ability of picophytoplankton to produce TEPs: Deng et al. (2016) found that *Synechococcus* could produce TEPs in a laboratory study; Iuculano et al. (2017) determined the production rates of TEPs by *Prochlorococcus* cells collected from the Atlantic and Pacific Oceans. A significant positive correlation was observed between TEPs and picophytoplankton biomass in both regions (Table 3), supporting the importance of picophytoplankton as an important TEP producer in oligotrophic tropical oceans. No significant correlation was observed between TEPs and HPs in this study (Table 3). Several previous studies have reported a significant positive correlation between these two variables (Corzo et al., 2005; Ortega-Retuerta et al., 2009, 2010; Dehwah et al., 2020), while others have not (Bhaskar and Bhosle, 2006; Zamanillo et al., 2019a). The effect of HPs on TEP distribution is complex in the ocean. On the one hand, they can stimulate the release of TEP precursors by phytoplankton cells and themselves could also release significant amounts of TEP precursors as capsular material (Passow, 2002a, b; Ortega-Retuerta et al., 2010, 2019). On the other hand, TEPs can be efficiently utilized by particle-attached bacteria relative to other components of POC (Zäncker

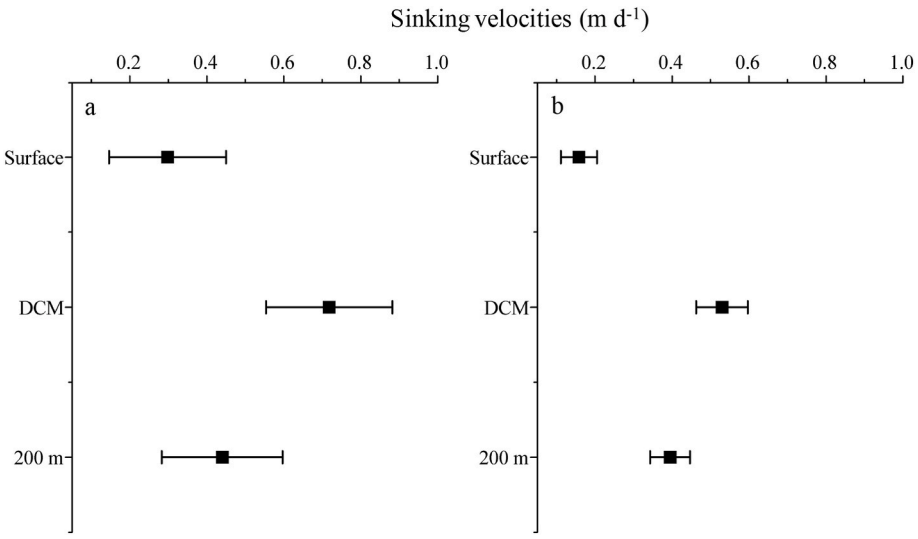

Fig. 6. The mean of sinking velocities of TEPs (m d^{-1}) in the surface, DCM and 200 m layer in the SCS (a) and WTNP (b). The error bar represents the standard devision.

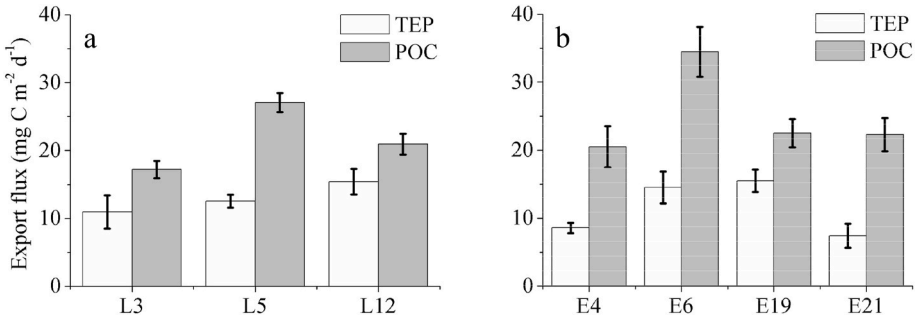

Fig. 7. Sinking flux of TEPs and POC in the SCS (a) and WTNP (b). The error bar represents the standard deviation.

Table 4
Comparison of TEP concentrations in this study with those in other studies in the oligotrophic ocean. nd: no data.

Location	Depth (m)	TEP range (μg Xeq. L^{-1})	TEP mean ± SD (μg Xeq. L^{-1})	Chl *a* (μg L^{-1})	Reference
Northeast Atlantic Ocean	0–50	10–120	29 ± 10	0–1.2	Engel, 2004
Mediterranean Sea	0–200	4–95	21	0–1.78	Ortega-Retuerta et al. (2010)
tropical North Pacific	5–300	18–69	42 ± 9	0–0.3	Kodama et al. (2014)
Sargasso Sea	0–100	21–57	nd	nd	Cisternas-Novoa et al., 2016
Equatorial Pacific Ocean	3	nd	24 ± 2	0–0.31	Iuculano et al. (2017)
NW Mediterranean Sea	4–200	5–55	19 ± 11	0.10–0.65	Ortega-Retuerta et al. (2017)
Pacific Ocean	0–200	5–40	25 ± 7	0–1.4	Yamada et al. (2017)
Mediterranean Sea and the North Eastern Atlantic Ocean	0–200	5–82	31	0–0.92	Ortega-Retuerta et al. (2019)
Atlantic Ocean	4	18–132	60 ± 27	0.2–0.41	Zamanillo et al. (2019a)
Eastern Indian Ocean	0–200	5–46	20 ± 6	0.23 ± 0.20	Guo et al. (2021)
Northern South China Sea	0–3700	0–79	nd	0–1.2	Ge et al. (2022)
South China Sea	0–220	14–47	30 ± 8	0–1.13	This study
Western tropical North Pacific	0–220	12–54	34 ± 10	0–0.44	This study

et al., 2019; Ge et al., 2022). Therefore, all these processes with different magnitudes and timescales would occur simultaneously in the environment, leading to the lack of consistency in the relationships between TEPs and HPs in this study, which highlights the complexity of the TEP-HP relationship in the ocean. Maximum values of TEPs concentrations were located between the surface and the DCM layer (Fig. 4), and TEP concentrations in the epipelagic layer were obviously higher than those in the deeper layer in both the SCS and WTNP (Fig. 4). Several studies in the oligotrophic open ocean have found similar distribution patterns (Ortega-Retuerta et al., 2017, 2019; Guo et al., 2021), and these observations establish that the accumulation of TEPs in the epipelagic layer is very common in the open ocean.

TEP concentrations correlated significantly positively with temperature in the SCS and WTNP in this study (Table 3). Several studies have examined the effects of temperature on TEP production by phytoplankton cells (Claquin et al., 2008; Fukao et al., 2012; Chen et al., 2021). Claquin et al. (2008) observed accelerated TEP production of several diatom species with increasing temperature in the range of 5–35 °C. Fukao et al. (2012) found that temperature could influence TEP production in *Coscinodiscus granii* cells by affecting their photosynthetic

activity. Chen et al. (2021) found that a temperature increase would promote TEPs formation by the diatom species *Skeletonema marinoi* and *Thalassiosira weissflogii*. The effect of temperature on TEP production in phytoplankton cells might be related to their carbohydrate allocation. The enzyme activity related to TEP production mechanisms of phytoplankton cells would be elevated as temperature increases, leading to increased excretion of phytoplankton extracellular carbohydrates, which are precursors of TEPs in the ocean (Zlotnik and Dubinsky, 1989; Wolfstein and Stal, 2002). It should be noted that most previous studies on the effect of temperature on TEP production were carried out in the laboratory, where temperature is the sole variable with other environmental parameters (e.g., nutrients, light) being stable (Claquin et al., 2008; Fukao et al., 2012; Chen et al., 2021), and this was quite different from the conditions in the field. Whether higher seawater temperatures could accelerate TEP production in oligotrophic tropical oceans deserves further study.

4.3. TEP-C contributed significantly to the POC pool and POC sinking flux

As TEPs are a constituent of the POC pool, expressing their concentrations in terms of carbon is important for determining the role of TEPs in organic carbon cycling in the ocean. TEP-C ranged from 7 to 24 μg C L^{-1} in the SCS and 6–28 μg C L^{-1} in the WTNP in this study, falling within the lower range of previously reported TEP-C values (2–800 μg C L^{-1}) from different oceanic environments (Engel and Passow, 2001). The percentage of POC attributed to TEPs averaged 75% in the SCS and 61% in the WTNP, which were higher than the TEP-C%POC values in the Atlantic Ocean (18%, Engel, 2004; 12%, Harlay et al., 2009) and the West Coast of India (6.88%, Bhaskar and Bhosle, 2006), lower than those in the Arctic Ocean (134%, Yamada et al., 2015; 160%, Yamada et al., 2017), and similar to those in the Eastern Mediterranean Sea (60–100%, Bar-Zeev et al., 2011). When compared with phytoplankton and HPs, TEPs contributed more to the POC pool in this study (Fig. 5), which was consistent with the study of Zamanillo et al. (2019a) in the open Atlantic Ocean. In several eutrophic systems, however, phytoplankton were reported to constitute the largest part of POC (Bhaskar and Bhosle, 2006; Ortega-Retuerta et al., 2009; Annane et al., 2015) when compared with TEPs and HPs. The high TEP-C%POC values in this study were mostly related to nutrient limitation in the SCS and WTNP, which would favor TEP production by phytoplankton cells and limit TEP consumption by HP (Iuculano et al., 2017). Generally, the results of this study suggest that TEPs and phytoplankton cells could constitute a majority of the POC pool in the SCS and WTNP.

To date, several studies have reported sinking velocities of TEPs in the lab. Azetsu-Scott and Passow (2004) determined the sinking velocities of freshly produced, particle-free TEPs and found that particle-free TEPs ascended with an average velocity of 0.14 m d^{-1}. Mari (2008) studied the effect of seawater acidification on the sinking behavior of TEPs and reported that TEP sinking velocities averaged 0.49 ± 0.37 m d^{-1}. Guo et al. (2021) determined sinking velocities of TEPs in the Eastern Indian Ocean with the SETCOL method, with sinking velocities ranging from −0.3 to 1.9 m d^{-1}. The 0.09–0.93 m d^{-1} range of TEP sinking velocities determined with the SETCOL method in this study was consistent with those of previous studies (Mari, 2008; Guo et al., 2021). It should be noted that the sinking velocities of TEP determined with the SETCOL method only represent the settling behavior of TEPs in the absence of turbulence. In the natural marine environment, the sinking velocities of TEPs should be the sum effect of their intrinsic sinking behavior and the turbulence of seawater. Nevertheless, the SETCOL-determined sinking velocity of TEPs in this study proves that TEPs have a potential to sink down when excluding the effect of seawater turbulence. The SETCOL-determined sinking velocities of TEPs were higher in the DCM layer than in the surface and 200 m layers in both regions (Fig. 6). According to coagulation theory, the aggregation of particles in the ocean is controlled by their concentrations and collision rates (Prieto et al., 2002; Burd and Jackson, 2009). In the DCM layer, high phytoplankton biomass would promote the collision rate between TEPs and phytoplankton cells, further accelerating the sinking of TEPs via the formation of fast-sinking TEP-phytoplankton aggregates (Vicente et al., 2009; Mari et al., 2017).

As the molar C: N ratios of TEPs (C: N = ~26) were above the Redfield ratio (C: N = 6.6:1) (Engel and Passow, 2001), sedimentation of TEPs could contribute to carbon export in the ocean directly (Martin et al., 2011). Therefore, knowledge of the relationship between TEPs and POC sinking flux is important for us to study the carbon cycle in the ocean. Most studies on the sinking flux of TEPs have been carried out in middle- and high-latitude oceans, such as the Santa Barbara Channel (Passow et al., 2001), the western subarctic Pacific (Ramaiah et al., 2005), and the subpolar North Atlantic (Martin et al., 2011), and few study has been carried out in oligotrophic tropical oceans (Ge et al., 2022). This study reported the sinking flux of TEPs in the SCS and WTNP, and it averaged 13 ± 2 mg C m^{-2} d^{-1} in the SCS and 12 ± 4 mg C m^{-2} d^{-1} in the WTNP, which was in accordance with that reported in the Santa Barbara Channel (from 7 to 70 mg C m^{-2} d^{-1}, Passow et al., 2001) and a Swedish fjord (up to 25 mg C m^{-2} d^{-1}, Waite et al., 2005), lower than that in the subarctic Pacific (from 29 to 62 mg C m^{-2} d^{-1}, Ramaiah et al., 2005) and the subpolar North Atlantic (up to 120 mg C m^{-2} d^{-1}, Martin et al., 2011), and higher than that in the Southern Ocean (≤2.5 mg C m^{-2} d^{-1}, Ebersbach et al., 2014). The carbon flux of TEPs accounted for 61% of the POC flux in the SCS and 46% in the WTNP, indicating that sinking TEPs constitute an important portion of POC export in these areas. According to increased greenhouse gases and aerosols, the oceanic temperature will continue to rise (Sarmiento et al., 2004), and the area of oligotrophic oceans will expand with the associated oceanic stratification in tropical/subtropical areas in the future (Bopp et al., 2013). As elevated nutrient stress levels and temperatures have been proven to stimulate the carbon overflow of phytoplankton cells and TEP production (Pedrotti et al., 2010; Fukao et al., 2012; Chen et al., 2021), the export of TEPs in these regions will play an increasingly important role in carbon export in the future.

4.4. Shortcomings of this study

Due to methodological limitations, the comparison of TEP-C and POC should be interpreted with caution in this study. TEP-C was estimated using a conversion factor (0.51 μg C [μg Xeq.]$^{-1}$) determined mainly by diatom cultures (Engel and Passow, 2001), and this conversion factor has also been used in the western North Atlantic Ocean (Jennings et al., 2017; Zamanillo et al., 2019a), the Mediterranean Sea (Ortega-Retuerta et al., 2018) and the Southern Ocean (Zamanillo et al., 2019b). In the SCS and WTNP, the phytoplankton community structure was mainly dominated by picophytoplankton (Chen et al., 2011, 2017), which was quite different from the phytoplankton groups (mainly diatoms) used in the experiments of Engel and Passow (2001). Therefore, whether the conversion factor for TEP-C estimation from Engel and Passow (2001) should be suitable for application in this study remains questionable, and there is a need to define specific TEP-to-carbon conversion factors for diverse regions with different environmental conditions. In the SCS and WTNP, high TEP-C%POC values exceeding 100% were observed (Fig. 5), which was impossible by definition, and this has also been observed in other studies (Bar-Zeev et al., 2011; Parinos et al., 2017; Ortega-Retuerta et al., 2019). If large quantities of small TEPs (<0.7 μm) passed through the GF/F filters for POC collection but were retained on the polycarbonate filters (0.4 μm) for TEP collection, this would result in the overestimation of TEP-C%POC. The export fluxes of TEP and POC were determined with short-term sediment traps in this study, which were also used by other studies (Kiørboe et al., 1998; Caron et al., 2004; Guo et al., 2010). The application of short-term sediment traps may bring some source of bias.

5. Conclusions

In conclusion, our study expands the existing knowledge on TEP concentrations and distributions in the SCS and WTNP and provides the information on the contribution of sinking TEPs to carbon export in these areas. TEP concentrations were higher in the epipelagic layer than in deeper layers in both regions, which was mostly due to the high phytoplankton biomass and nutrient shortage in the epipelagic layer. TEPs constituted a large portion of the POC pool in both the SCS and WTNP, larger than phytoplankton cells and heterotrophic prokaryotes, supporting the important role of TEPs in the carbon cycle in both regions. The SETCOL-determined sinking velocities of TEPs were not constant but varied considerably in the euphotic zone, and they were higher in the DCM layer than in the surface and 200 m layers. High phytoplankton biomass would promote the collision rate between TEPs and phytoplankton cells, forming fast-sinking TEP-phytoplankton aggregates, which should be responsible for the high SETCOL-determined sinking velocities of TEPs in the DCM layer. The carbon flux of TEPs accounted for 61% of the POC flux in the SCS and 46% in the WTNP, highlighting the important role of TEPs sinking in carbon export in these areas. This underscores the necessity for future studies to clarify the contribution of TEPs to organic carbon fluxes in oligotrophic tropical oceans, which occupy a large part of the global ocean.

Data availability statement

Data supporting these findings can be found online at Mendeley Data, https://doi.org/10.17632/r92hwc8g76.1.

Author statement

Shujin Guo: Conceptualization, Methodology, Investigation, Data Curation, Writing-Original Draft, Writing-Review & Editing, Visualization.

Ying Wu: Investigation, Data Curation.

Mingliang Zhu: Investigation, Resources.

Xiaoxia Sun: Conceptualization, Supervision, Funding acquisition.

Declaration of competing interest

The authors declare that they have no known competing financial interests or personal relationships that could have appeared to influence the work reported in this paper.

Acknowledgement

This work was supported by the International Science Partnership Program of the Chinese Academy of Sciences (No. 121311KYSB20190029), the National Natural Science Foundation of China (No. 31700425), the Strategic Priority Research Program of the Chinese Academy of Sciences (No. XDB42000000), the Natural Basic Research Program of China (No. 2014CB441504), the International Science Partnership Program of the Chinese Academy of Sciences (No. 133137KYSB20200002), and the Taishan Scholars Project to SUN Song. Data and samples in the western tropical North Pacific were collected onboard R/V “Ke Xue”, implementing the open research cruise NORC2019-09 supported by NSFC Shiptime Sharing Project (No. 41849909). The authors also thank all the crews in “Nanfeng” for their support in the sample collection.

References

Alldredge, A.L., Passow, U., Logan, B.E., 1993. The abundance and significance of a class of large, transparent organic particles in the ocean. Deep-Sea Res. I 40 (6), 1131–1140.

Annane, S., St-Amand, L., Starr, M., Pelletier, E., Ferreyra, G.A., 2015. Contribution of transparent exopolymer particles (TEP) to estuarine particulate organic carbon pool. Mar. Ecol. Prog. Ser. 529, 17–34.

Azetsu-Scott, K., Passow, U., 2004. Ascending marine particles: significance of transparent exopolymer particles (TEP) in the upper ocean. Limnol. Oceanogr. 49, 741–748.

Bar-Zeev, E., Berman-Frank, I., Stambler, N., Domínguez, E.V., Zohary, T., Capuzzo, E., Meeder, E., Suggett, D.J., Iluz, D., Dishon, G., Berman, T., 2009. Transparent exopolymer particles (TEP) link phytoplankton and bacterial production in the Gulf of Aqaba. Aquat. Microb. Ecol. 56, 217–225.

Bar-Zeev, E., Berman, T., Rahav, E., Dishon, G., Herut, B., Kress, N., Berman-Frank, I., 2011. Transparent exopolymer particle (TEP) dynamics in the eastern Mediterranean Sea. Mar. Ecol. Prog. Ser. 431, 107–118.

Beauvais, S., Pedrotti, M.L., Egge, J., Iversen, K., Marrasé, C., 2006. Effects of turbulence on TEP dynamics under contrasting nutrient conditions: implications for aggregation and sedimentation processes. Mar. Ecol. Prog. Ser. 323, 47–57.

Bhaskar, P.V., Bhosle, N.B., 2006. Dynamics of transparent exopolymeric particles (TEP) and particle-associated carbohydrates in the Dona Paula bay, west coast of India. J. Earth Syst. Sci. 115, 403–413.

Bienfang, P.K., 1981. SETCOL—a technologically simple and reliable method for measuring phytoplankton sinking rates. Can. J. Fish. Aquat. Sci. 38 (10), 1289–1294.

Bopp, L., Resplandy, L., Orr, J.C., Doney, S.C., Dunne, J.P., Gehlen, M., Halloran, P., Heinze, C., Ilyina, T., Séférian, R., 2013. Multiple stressors of ocean ecosystems in the 21st century: projections with CMIP5 models. Biogeosciences 10, 6225–6245.

Burd, A.B., Jackson, G.A., 2009. Particle aggregation. Ann. Rev. Mar. Sci 1, 65–90.

Burns, W.G., Marchetti, A., Ziervogel, K., 2019. Enhanced formation of transparent exopolymer particles (TEP) under turbulence during phytoplankton growth. J. Plankton Res. 41 (3), 349–361.

Caron, G., Michel, C., Gosselin, M., 2004. Seasonal contributions of phytoplankton and fecal pellets to the organic carbon sinking flux in the North Water (northern Baffin Bay). Mar. Ecol. Prog. Ser. 283, 1–13.

Chen, B.Z., Wang, L., Song, S.Q., Huang, B.Q., Sun, J., Liu, H.B., 2011. Comparisons of picophytoplankton abundance, size, and fluorescence between summer and winter in northern South China Sea. Continent. Shelf Res. 31 (14), 1527–1540.

Chen, J., Guo, K.L., Thornton, D.C.O., Wu, Y., 2021. Effect of temperature on the release of transparent exopolymer particles (TEP) and aggregation by marine diatoms (*Thalassiosira weissflogii* and *Skeletonema marinoi*). J. Ocean Univ. China 20 (1), 56–66.

Chen, Y.Y., Sun, X.X., Zhu, M.L., Zheng, S., Yuan, Y.Q., Denis, M., 2017. Spatial variability of phytoplankton in the Pacific western boundary currents during summer 2014. Mar. Freshw. Res. 68 (10), 1887–1900.

Christian, J.R., Feely, R.A., Ishii, M., Murtugudde, R., Wang, X.J., 2008. Testing an ocean carbon model with observed sea surface pCO_2 and dissolved inorganic carbon in the tropical Pacific Ocean. J. Geophys. Res. 113, C07047.

Cisternas-Novoa, C., Lee, C., Engel, A., 2016. Transparent exopolymer particles (TEP) and Coomassie stainable particles (CSP): differences between their origin and vertical distributions in the ocean. Mar. Chem. 175, 56–71.

Claquin, P., Probert, I., Lefebvre, S., Veron, B., 2008. Effects of temperature on photosynthetic parameters and TEP production in eight species of marine microalgae. Aquat. Microb. Ecol. 51, 1–11.

Corzo, A., Rodríguez-Gálvez, S., Lubian, L., Sangrá, P., Martínez, A., Morillo, J.A., 2005. Spatial distribution of transparent exopolymer particles in the Bransfield Strait, Antarctica. J. Plankton Res. 27, 635–646.

Dai, S., Zhao, Y.F., Li, X.G., Wang, Z.Y., Zhu, M.L., Liang, J.H., Liu, H.J., Tian, Z.Y., Sun, X.X., 2020. The seamount effect of phytoplankton in the tropical western Pacific. Mar. Environ. Res. 162, 105094.

Deng, W., Cruz, B.N., Neuer, S., 2016. Effects of nutrient limitation on cell growth, TEP production and aggregate formation of marine *Synechococcus*. Aquat. Microb. Ecol. 78, 39–49.

Dehwah, A.H.A., Anderson, D.M., Li, S., Mallon, F.L., Batang, Z., Alshahri, A.H., Tsegaye, S., Hegy, M., Missimer, T.M., 2020. Understanding transparent exopolymer particle occurrence and interaction with algae, bacteria, and the fractions of natural organic matter in the Red Sea: implications for seawater desalination. Desalination Water Treat. 192, 78–96.

Ducklow, H., 2000. Bacterial production and biomass in the oceans. In: Kirchman, D.L. (Ed.), Microbial Ecology of the Oceans. Wiley, New York, pp. 104–108.

Ebersbach, F., Assmy, P., Martin, P., Schulz, I., Wolzenburg, S., Nöthig, E.M., 2014. Particle flux characterization and sedimentation patterns of protistan plankton during the iron fertilization experiment LOHAFEX in the Southern Ocean. Deep-Sea Res. I 89, 94–103.

Engel, A., Passow, U., 2001. Carbon and nitrogen content of transparent exopolymer particles (TEP) in relation to their Alcian Blue adsorption. Mar. Ecol. Prog. Ser. 219, 1–10.

Engel, A., 2004. Distribution of transparent exopolymer particles (TEP) in the northeast Atlantic Ocean and their potential significance for aggregation processes. Deep-Sea Res. I 51, 83–92.

Fukao, T., Kimoto, K., Kotani, Y., 2012. Effect of temperature on cell growth and production of transparent exopolymer particles by the diatom *Coscinodiscus granii* isolated from marine mucilage. J. Appl. Phycol. 24, 181–186.

Ge, Z.M., Li, Q.P., Yang, W.F., Liu, X., Wu, Z.C., 2022. Transparent exopolymer particle dynamics along a shelf-to-sea gradient and impacts on the regional carbon cycle. Sci. Total Environ. 808, 152117.

Guo, C.C., Sun, J., Wang, X.Z., Jian, S., Noman, M.A., Huang, K., Zhang, G.C., 2021. Distribution and settling regime of transparent exopolymer particles (TEP) potentially associated with bio-physical processes in the Eastern Indian Ocean. J. Geophys. Res. 126 (4), e2020JG005934.

Guo, S.J., Sun, X.X., 2019. Concentrations and distribution of transparent exopolymer particles in a eutrophic coastal sea: a case study of the Changjiang (Yangtze River) estuary. Mar. Freshw. Res. 70 (10), 1389–1401.
Guo, X.W., Zhang, Y.S., Zhang, F.J., Cao, Q.Y., 2010. Characteristics and flux of settling particulate matter in neritic waters: the southern Yellow Sea and the East China Sea. Deep-Sea Res. II 57, 1058–1063.
Han, A.Q., Dai, M.H., Kao, S.J., Gan, J.P., Li, Q., Wang, L.F., Zhai, W.D., Wang, L., 2012. Nutrient dynamics and biological consumption in a large continental shelf system under the influence of both a river plume and coastal upwelling. Limnol. Oceanogr. 57 (2), 486–502.
Harlay, J., De Bodt, C., Engel, A., Jansen, S., d'Hoop, Q., Piontek, J., Oostende, N.V., Groom, S., Sabbe, K., Chou, L., 2009. Abundance and size distribution of transparent exopolymer particles (TEP) in a coccolithophorid bloom in the northern Bay of Biscay. Deep-Sea Res. I 56, 1251–1265.
Heinonen, K.B., Ward, J.E., Holohan, B.A., 2007. Production of transparent exopolymer particles (TEP) by benthic suspension feeders in coastal systems. J. Exp. Mar. Biol. Ecol. 341 (2), 184–195.
Hillebrand, H., Dürselen, C.D., Kirschtel, D., Pollingher, U., Zohary, T., 1999. Biovolume calculation for pelagic and benthic microalgae. J. Phycol. 35, 403–424.
Iuculano, F., Mazuecos, I.P., Reche, I., Agustí, S., 2017. *Prochlorococcus* as a possible source for transparent exopolymer particles (TEP). Front. Microbiol. 8, 709.
Jennings, M.K., Passow, U., Wozniak, A.S., Hansell, D.A., 2017. Distribution of transparent exopolymer particles (TEP) across an organic carbon gradient in the western North Atlantic Ocean. Mar. Chem. 190, 1–12.
Kiørboe, T., Tiselius, P., Mitchell-Innes, B., Hansen, J.L.S., Visser, A.W., Mari, X., 1998. Intensive aggregate formation with low vertical flux during an upwelling-induced diatom bloom. Limnol. Oceanogr. 43 (1), 104–116.
Kodama, T., Kurogi, H., Okazaki, M., Jinbo, T., Chou, S., Tomoda, T., Ichikawa, T., Watanabe, T., 2014. Vertical distribution of transparent exopolymer particle (TEP) concentration in the oligotrophic western tropical North Pacific. Mar. Ecol. Prog. Ser. 513, 29–37.
Koeve, W., 2005. Magnitude of excess carbon sequestration into the deep ocean and the possible role of TEP. Mar. Ecol. Prog. Ser. 291, 53–64.
Li, X.Y., Passow, U., Logan, B.E., 1998. Fractal dimensions of small (15-200 μm) particles in Eastern Pacific coastal waters. Deep-Sea Res. I 45 (1), 115–131.
Li, Q.P., Ge, Z.M., Liu, Z.J., Zhou, W.W., Shuai, Y.P., Wu, Z.C., 2021. Transparent exopolymer particles in a coastal frontal zone of the northern South China Sea and the associated biogeochemical implications. J. Geophys. Res. 126, e2020JG005893.
Liu, F.F., Tang, S.L., Huang, R.X., Yin, K.D., 2017. The asymmetric distribution of phytoplankton in anticyclonic eddies in the western South China Sea. Deep-Sea Res. I 120, 29–38.
Liu, Q., Zhao, Q.N., Jiang, Y., Li, Y., Zhang, C.R., Li, X.R., Yu, X.W., Huang, L.Y., Wang, M., Yang, G.P., Chen, H.T., Tian, J.W., 2021a. Diversity and co-occurrence networks of picoeukaryotes as a tool for indicating underlying environmental heterogeneity in the Western Pacific Ocean. Mar. Environ. Res. 170, 105376.
Liu, Z.J., Li, Q.P., Ge, Z.M., Shuai, Y.P., 2021b. Variability of plankton size distribution and controlling factors across a coastal frontal zone. Prog. Oceanogr. 197, 102665.
Ma, J., Song, J.M., Li, X.G., Wang, Q.D., Sun, X.X., Zhang, W.C., Zhong, G.R., 2021. Seawater stratification vs. plankton for oligotrophic mechanism: a case study of M4 seamount area in the Western Pacific Ocean. Mar. Environ. Res. 169, 105400.
Mari, X., 2008. Does ocean acidification induce an upward flux of marine aggregates? Biogeosci. Discuss. 5, 1631–1654.
Mari, X., Passow, U., Migon, C., Burd, A.B., Legendre, L., 2017. Transparent exopolymer particles: effects on carbon cycling in the ocean. Prog. Oceanogr. 151, 13–37.
Martin, P., Lampitt, R.S., Perry, M.J., Sanders, R., Lee, C., D'Asaro, E., 2011. Export and mesopelagic particle flux during a North Atlantic spring diatom bloom. Deep-Sea Res. I 58, 338–349.
Menden-Deuer, S., Lessard, E.J., 2000. Carbon to volume relationships for dinoflagellates, diatoms, and other protist plankton. Limnol. Oceanogr. 45, 569–579.
Messié, M., Radenac, M.H., 2006. Seasonal variability of the surface chlorophyll in the western tropical Pacific from SeaWiFS data. Deep-Sea Res. I 53, 1581–1600.
Morelle, J., Schapira, M., Claquin, P., 2017. Dynamics of phytoplankton productivity and exopolysaccharides (EPS and TEP) pools in the Seine Estuary (France, Normandy) over tidal cycles and over two contrasting seasons. Mar. Environ. Res. 131, 162–176.
Moutin, T., Karl, D.M., Duhamel, S., Rimmelin, P., Raimbault, P., Van Mooy, B.A.S., Claustre, H., 2008. Phosphate availability and the ultimate control of new nitrogen input by nitrogen fixation in the tropical Pacific Ocean. Biogeosciences 5, 95–109.
Nissimov, J.I., Vandzura, R., Johns, C.T., Natale, F., Haramaty, L., Bidle, K.D., 2018. Dynamics of transparent exopolymer particle (TEP) production and aggregation during viral infection of the coccolithophore, *Emiliania huxleyi*. Environ. Microbiol. 20 (8), 2880–2897.
Obernosterer, I., Herndl, G.J., 1995. Phytoplankton extracellular release and bacterial growth: dependence on inorganic N:P ratio. Mar. Ecol. Prog. Ser. 116, 247–257.
Ortega-Retuerta, E., Reche, I., Pulido-Villena, E., Agustí, S., Duarte, C.M., 2009. Uncoupled distributions of transparent exopolymer particles (TEP) and dissolved carbohydrates in the Southern Ocean. Mar. Chem. 115, 59–65.
Ortega-Retuerta, E., Duarte, C.M., Reche, I., 2010. Significance of bacterial activity for the distribution and dynamics of transparent exopolymer particles in the Mediterranean Sea. Microb. Ecol. 59, 808–818.
Ortega-Retuerta, E., Sala, M.M., Borrull, E., Mestre, M., Aparicio, F.L., Gallisai, R., Antequera, C., Marrasé, C., Peters, F., Simó, R., Gasol, J.M., 2017. Horizontal and vertical distributions of transparent exopolymer particles (TEP) in the NW Mediterranean Sea are linked to chlorophyll *a* and O_2 variability. Front. Microbiol. 7, 2159.
Ortega-Retuerta, E., Marrasé, C., Muñoz-Fernández, A., Sala, M.M., Simó, R., Gasol, J.M., 2018. Seasonal dynamics of transparent exopolymer particles (TEP) and their drivers in the coastal NW Mediterranean Sea. Sci. Total Environ. 631, 180–190.
Ortega-Retuerta, E., Mazuecos, I.P., Reche, I., Gasol, J.M., Álvarez-Salgado, X.A., Álvarez, M., Montero, M.F., Arístegui, J., 2019. Transparent exopolymer particle (TEP) distribution and in situ prokaryotic generation across the deep Mediterranean Sea and nearby North East Atlantic Ocean. Prog. Oceanogr. 173, 180–191.
Palmer, J.R., Totterdell, I.J., 2001. Production and export in a global ocean ecosystem model. Deep-Sea Res. I 48 (5), 1169–1198.
Parinos, C., Gogou, A., Krasakopoulou, E., Lagaria, A., Giannakourou, A., Karageorgis, A. P., Psarra, S., 2017. Transparent exopolymer particles (TEP) in the NE Aegean Sea frontal area: seasonal dynamics under the influence of Black Sea water. Continent. Shelf Res. 149, 112–123.
Passow, U., Alldredge, A.L., 1995a. A dye-binding assay for the spectrophotometric measurement of transparent exopolymer particles (TEP). Limnol. Oceanogr. 40, 1326–1335.
Passow, U., Alldredge, A.L., 1995b. Aggregation of a diatom bloom in a mesocosm: the role of transparent exopolymer particles (TEP). Deep-Sea Res. II 42, 99–109.
Passow, U., Shipe, R.F., Murray, A., Pak, D.K., Brzezinski, M.A., Alldredge, A.L., 2001. The origin of transparent exopolymer particles (TEP) and their role in the sedimentation of particulate matter. Continent. Shelf Res. 21, 327–346.
Passow, U., 2002a. Transparent exopolymer particles (TEP) in aquatic environments. Prog. Oceanogr. 55, 287–333.
Passow, U., 2002b. Production of transparent exopolymer particles (TEP) by phyto- and bacterioplankton. Mar. Ecol. Prog. Ser. 236, 1–12.
Pedrotti, M.L., Peters, F., Beauvais, S., Vidal, M., Egge, J., Jacobsen, A., Marrasé, C., 2010. Effects of nutrients and turbulence on the production of transparent exopolymer particles: a mesocosm study. Mar. Ecol. Prog. Ser. 419, 57–69.
Ploug, H., Passow, U., 2007. Direct measurement of diffusivity within diatom aggregates containing transparent exopolymer particles. Limnol. Oceanogr. 52 (1), 1–6.
Prieto, L., Sommer, F., Stibor, H., Koeve, W., 2001. Effects of planktonic copepods on transparent exopolymeric particles (TEP) abundance and size spectra. J. Plankton Res. 23 (5), 515–525.
Prieto, L., Ruiz, J., Echevarría, F., García, C.M., Bartual, A., Gálvez, J.A., Corzo, A., Macías, D., 2002. Scales and processes in the aggregation of diatom blooms: high time resolution and wide size range records in a mesocosm. Deep-Sea Res. I 49 (7), 1233–1253.
Ramaiah, N., Takeda, S., Furuya, K., Yoshimura, T., Nishioka, J., Aono, T., Nojiri, Y., Imai, K., Kudo, I., 2005. Effect of iron enrichment on the dynamics of transparent exopolymer particles in the western subarctic Pacific. Prog. Oceanogr. 64, 253–261.
Sarmiento, J.L., Slater, R., Barber, R., Bopp, L., Doney, S.C., Hirst, A.C., Kleypas, J., Matear, R., Mikolajewicz, U., Monfray, P., Soldatov, V., Spall, S.A., Stouffer, R., 2004. Response of ocean ecosystems to climate warming. Global Biogeochem. Cycles 18 (3), GB3003.
Shackelford, R., Cowen, J.P., 2006. Transparent exopolymer particles (TEP) as a component of hydrothermal plume particle dynamics. Deep-Sea Res. I 53 (10), 1677–1694.
Sugimoto, K., Fukuda, H., Baki, M.A., Koike, I., 2007. Bacterial contributions to formation of transparent exopolymer particles (TEP) and seasonal trends in coastal waters of Sagami Bay, Japan. Aquat. Microb. Ecol. 46, 31–41.
Sun, C.C., Wang, Y.S., Li, Q.P., Yue, W.Z., Wang, Y.T., Sun, F.L., Peng, Y.L., 2012. Distribution characteristics of transparent exopolymer particles in the Pearl River estuary, China. J. Geophys. Res. 117, G00N17.
Underwood, G.J.C., Boulcott, M., Raines, C.A., Waldron, K., 2004. Environmental effects on exopolymer production by marine benthic diatoms: dynamics, changes in composition and pathways of production. J. Phycol. 40, 293–304.
Utermöhl, H., 1958. Zur Vervollkommnung der quantitative phytoplankton-Methodik. In: Mitteilungen der Internationale Vereinigung für Limnologie, Mitteilungen, 9, pp. 1–38.
Vicente, I.D., Ortega-Retuerta, E., Romera, O., Morales-Baquero, R., Reche, I., 2009. Contribution of transparent exopolymer particle to carbon sinking flux in an oligotrophic reservoir. Biogeochemistry 96 (1–3), 13–23.
Waite, A.M., Gustafsson, Ö., Lindahl, O., Tiselius, P., 2005. Linking ecosystem dynamics and biogeochemistry: sinking fractionation of organic carbon in a Swedish fjord. Limnol. Oceanogr. 50 (2), 658–671.
Welschmeyer, N.A., 1994. Fluorometric analysis of chlorophyll *a* in the presence of chlorophyll *b* and pheopigments. Limnol. Oceanogr. 39 (8), 1985–1992.
Wolfstein, K.L., Stal, J., 2002. Production of extracellular polymeric substances (EPS) by benthic diatoms: effect of irradiance and temperature. Mar. Ecol. Prog. Ser. 236, 13–22.
Xiao, P., Jiang, Y.G., Liu, Y., Tan, W.H., Li, W.H., Li, R.H., 2015. Re-evaluation of the diversity and distribution of diazotrophs in the South China Sea by pyrosequencing the *nifH* gene. Mar. Freshw. Res. 66 (8), 681–691.
Yamada, Y., Fukuda, H., Uchimiya, M., Motegi, C., Nishino, S., Kikuchi, T., Nagata, T., 2015. Localized accumulation and a shelf-basin gradient of particles in the Chukchi Sea and Canada Basin, western Arctic. J. Geophys. Res. 120, 4638–4653.
Yamada, Y., Yokokawa, T., Uchimiya, M., Nishino, S., Fukuda, H., Ogawa, H., Nagata, T., 2017. Transparent exopolymer particles (TEP) in the deep ocean: full-depth distribution patterns and contribution to the organic carbon pool. Mar. Ecol. Prog. Ser. 583, 81–93.
Zäncker, B., Engel, A., Cunliffe, M., 2019. Bacterial communities associated with individual transparent exopolymer particles (TEP). J. Plankton Res. 41 (4), 561–565.

Zamanillo, M., Ortega-Retuerta, E., Nunes, S., Rodríguez-Ros, P., Dall'Osto, M., Estrada, M., Sala, M.M., Simó, R., 2019a. Main drivers of transparent exopolymer particle distribution across the surface Atlantic Ocean. Biogeosciences 16, 733–749.
Zamanillo, M., Ortega-Retuerta, E., Nunes, S., Estrada, M., Sala, M.M., Royer, S.J., López-Sandoval, D.C., Emelianov, M., Vaqué, D., Marrasé, C., Simó, R., 2019b. Distribution of transparent exopolymer particles (TEP) in distinct regions of the Southern Ocean. Sci. Total Environ. 691, 736–748.
Zlotnik, I., Dubinsky, Z., 1989. The effect of light and temperature on DOC excretion by phytoplankton. Limnol. Oceanogr. 34, 831–839.